

# Quantum advantage of time-reversed ancilla-based metrology of absorption parameters

Jiaxuan Wang,<sup>1,2</sup> Ruynet. L. de Matos Filho,<sup>3</sup> Girish S. Agarwal,<sup>1,2,4</sup> and Luiz Davidovich<sup>1,2,3</sup>

<sup>1</sup>*Department of Physics and Astronomy, Texas A&M University, College Station, Texas 77843, USA*

<sup>2</sup>*Institute for Quantum Science and Engineering, Texas A&M University, College Station, Texas 77843, USA*

<sup>3</sup>*Instituto de Física, Universidade Federal do Rio de Janeiro, Rio de Janeiro, RJ 21941-972, Brazil*

<sup>4</sup>*Department of Biological and Agricultural Engineering,  
Texas A&M University, College Station, Texas 77843, USA*

Quantum estimation of parameters defining open-system dynamics may be enhanced by using ancillas that are entangled with the probe but are not submitted to the dynamics. Here we consider the important problem of estimation of transmission of light by a sample, with losses due to absorption and scattering. We show, through the determination of the quantum Fisher information, that the ancilla strategy leads to the best possible precision in single-mode estimation – the one obtained for a Fock state input –, through joint photon-counting of probe and ancilla, which are modes of a bimodal squeezed state produced by an optical parametric amplifier. This proposal overcomes the challenge of producing and detecting high photon-number Fock states, and it is quite robust against additional noise: we show that it is immune to phase noise and the precision does not change if the incoming state gets disentangled. Furthermore, the quantum gain is still present under moderate photon losses of the input beams. We also discuss an alternative to joint photon counting, which is readily implementable with present technology, and approaches the quantum Fisher information result for weak absorption, even with moderate photons losses of the input beams before the sample is probed: a time-reversal procedure, placing the sample between two optical parametric amplifiers, with the second undoing the squeezing produced by the first one. The precision of estimation of the loss parameter is obtained from the average outgoing total photon number and its variance. In both procedures, the state of the probe and the detection procedure are independent of the value of the parameter.

## I. INTRODUCTION

Quantum sensing involves the use of quantum resources, like entanglement and squeezing, for the estimation of parameters characteristic of a physical process, through its action on a probe that, upon a proper measurement, allows the estimation of the value of the parameters [1, 2]. It has become one of the most active areas of quantum information, with important theoretical developments and useful devices [3]. Entanglement of the probe with an ancilla that is not submitted to the physical process may increase the precision of estimation [4, 5]. This is true, however, only to open-system dynamics. Here we apply the ancilla protocol to the estimation of the photon-loss coefficient of a sample, due to absorption and scattering of light. The probe and the ancilla correspond to two modes of a bimodal squeezed state, produced by an optical parametric amplifier (OPA). Relevant aspects of the ancilla protocol for estimating absorption were studied theoretically [6–8] and experimentally [9, 10]. Here we show, through a novel and clarifying analytical procedure, that, for a given input intensity through the sample, this scheme leads to precision of estimation identical to the best possible one for single-mode estimation, obtained by using Fock states [11–13]. This has the advantage of avoiding the preparation of Fock states with high photon numbers, though in principle such states can be heralded from a two-mode squeezed vacuum state via the use of photon-number resolving detectors, as demonstrated in [14] for up to five photons. Our derivation allows us to determine the corresponding best measurement: a joint photon-counting of the outgoing probe and the ancilla. Since this measurement could be challenging with current technologies, except for joint Fock-state spaces of very small size, we present a time-reversal detection alternative,

consisting in placing the sample between two bimodal squeezing transformations (two OPAs), such that the second squeezing is the inverse of the first one. The precision in the estimation of the loss parameter is obtained from the averaged total photon number and its variance after the second transformation.

Time-reversal has been shown to increase the precision of estimation of parameters characterizing unitary processes, beyond the classical limit, like displacements [15–18] and phases [18–22]. For absorption estimation, time-reversal must be complemented by the use of ancilla. We show that, for small absorption, the estimation obtained with this approach is very close to the best possible precision, obtained from single-mode probes prepared in a Fock state [12, 13], and it is superior to proposals based on a single probe (no ancilla), prepared in a squeezed state [11]. It has the further advantage that neither the input state nor the detection procedure depends on the value of the parameter, which simplifies the experimental realization, avoiding resource-consuming adaptive measurements, and should motivate useful applications. While adaptive strategies require additional measurements, they can be useful in several situations [23–26], and specially when the number of probes is small [27]. Our method, has the advantage of avoiding the adaptation of the apparatus throughout the measurement. We show that quantum advantage is still present under moderate photon losses of the input beam.

Measuring the probe, after it undergoes the parameter-dependent dynamics, leads to an estimation of the parameter through a function – an estimator – that maps an experimental data set to a possible value of the parameter. There are four basic questions that one would like to answer: (i) How to define the precision of the estimate?; (ii) How to get the precision from the experimental results?; (iii) What is the best

initial state of the probe, in order to get the best precision?; and (iv) What is the best measurement procedure?

For unbiased estimations, the average of the estimator over a large number of realizations of the measurement coincides with the true value of the parameter. In this case, the precision of the estimation may be quantified by the standard deviation of the measured values of the parameter with respect to the average:  $\Delta X = \sqrt{\langle X^2 \rangle - \langle X \rangle^2}$ . Within the classical framework, a lower bound for the variance was obtained by Cramér and Rao [28], and shown by Fisher [29] to be attainable when the distribution of the possible values of the parameter is Gaussian, or when the number of repetitions of the measurement is much larger than one. The Cramér-Rao bound is expressed in terms of the *Fisher information*,

$$F(X) = \sum_j \frac{1}{P_j(X)} \left[ \frac{dP_j(X)}{dX} \right]^2, \quad (1)$$

where  $P_j(X)$  is the probability of getting an experimental result  $j$  if the value of the parameter is  $X$ . One has then  $\Delta X \geq 1/\sqrt{NF(X)}$ , where  $N$  is the number of independent measurements.

Generalization of this early work to quantum mechanics, through maximization of  $F(X)$  over all possible quantum measurements, leads to the inequality

$$\Delta X \geq 1/\sqrt{N\mathcal{F}_Q(X)}, \quad (2)$$

where  $\mathcal{F}_Q(X)$  is the quantum Fisher information (QFI). This relation implies that the precision in the estimation of parameters can be increased beyond the minimum uncertainty obtained by classical means, usually referred to as the standard limit [1, 2, 30]. Quantum advantage has been proven for estimations of displacements or rotations [17, 18, 31–35], phases [36–42], electromagnetic fields [16, 34, 35, 43, 44], damping and temperature [11–13], the gravitational field [45–47], or yet the squeezing parameter of electromagnetic fields [48, 49]. More recently, interesting applications have been demonstrated, among them gravimeters [50], accelerometers [51], gyroscopes [52], magnetometers [53], high-resolution spectroscopy [54], detection of gravitational waves [32, 55], and ultra-precise atomic clocks [56]. Quantum metrology also concerns conceptual questions related to foundations of quantum mechanics, as, for instance, the meaning of number-phase and energy-time uncertainty relations [57], this last one being related to the quantum speed limit [58, 59].

For noiseless quantum processes, with probe dynamics governed by unitary evolution, and unbiased estimators, simple expressions are obtained for the quantum Cramér-Rao bound. This is not so, however, for open systems, that is, systems in the presence of an environment. Exact solutions can be found for one or two qubits [4, 5], but for higher dimensions it is not possible, in general, to find analytical solutions. Lower bounds for the variance can be found through purification of the non-unitary dynamics, by adding an ad hoc environment, such that the dynamics of the enlarged system is unitary and the reduced dynamics, obtained by tracing out the

added environment, coincides with the original dynamics of the system [41, 43, 59, 60]. Lower bounds for the precision have also been obtained via tools based on the geometry of quantum channels and semi-definite programming [61]. Also, exact solutions for the Cramér-Rao bound can be found for Gaussian systems [11, 62–64].

Parameter estimation is closely related to quantum channel identification, that is, the distinguishability of quantum channels upon a change of one or more of the parameters defining the channel [1]. In quantum information, a quantum channel is a completely positive trace-preserving map between spaces of operators, where a map  $\Gamma$  acting on operators in a Hilbert space  $\mathcal{H}_1$  is completely positive if the map  $\Gamma \otimes I$  is positive when acting on all possible extensions  $\mathcal{H}_1 \otimes \mathcal{H}_2$  of  $\mathcal{H}_1$ . It is known that entanglement of the probe with an ancilla, with the channel acting only on the probe, may improve parameter estimation and the discrimination of quantum channels [4, 5, 65–72]. The quantum advantage of this strategy is not universal, but it was demonstrated in some specific examples. In particular, it does not hold for unitary channels. Error correction, through the addition of multiple ancillas, has also been shown to increase the precision of estimation [73–75].

Here we consider the quantum sensing of photon loss, due to absorption and scattering by a material [6, 8–13, 76]. It has direct application to the estimation of the transmissivity of light by a sample, especially for weak losses, and when low intensities are desirable, which may be the case for fragile materials. Quantum metrology of absorption is also important in absorption imaging. Reference [77] demonstrated sub-shot noise quantum imaging using entangled photons produced by a down converter. Reference [78] demonstrated that the use of an ancilla in quantum illumination increases the signal-to-noise ratio beyond the classical value, in an entanglement-breaking environment.

The absorption constant  $\alpha$ , to be estimated, is defined so that, if  $I_0$  and  $I_1$  are the intensities of light before and after the absorbing sample, then  $I_1 = (1 - \alpha)I_0$ .

While we concentrate here on the estimation of the absorption from a single-mode probe, this strategy is of broader application. For instance, it can be extended to the important spectroscopic technique that determines differential absorption of two orthogonal polarized modes, which has recently been investigated [79, 80].

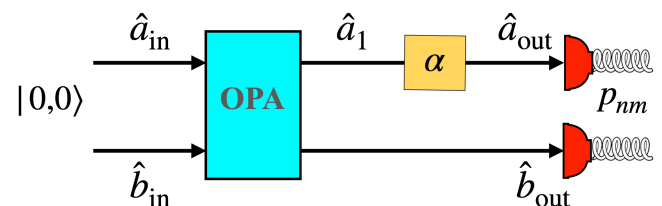


FIG. 1. Experimental setup for attaining a precision of estimation of an absorption coefficient  $\alpha$  equivalent to the one obtained by a Fock state, using however a bimodal squeezed state produced by an optical parametric amplifier as input. The estimation of  $\alpha$  is obtained from the joint photon counting of the two outgoing modes – probe plus ancilla.

## II. REACHING THE ULTIMATE PRECISION LIMIT

The ultimate precision limit for the estimation of absorption of a sample in the setup considered here is obtained through the quantum Fisher information for the system probe + ancilla, which corresponds to the signal and idler beams of a bimodal squeezed state, produced by an optical parametric amplifier (OPA). Since the input state is Gaussian, the techniques used in [11, 62–64] can be applied to this case. This is done in Appendix A. Here, we adopt, however, a different procedure, which clarifies the physical meaning of our results, and leads to the QFI derived in the Appendix.

The system to be considered is pictured in Fig. 1. The OPA implements a bimodal squeezing transformation  $\hat{S}(\xi)$  on a vacuum field [81],

$$\hat{S}(\xi) = \exp(\xi \hat{a}^\dagger \hat{b}^\dagger - \xi^* \hat{a} \hat{b}) \quad (3)$$

leading to the squeezed state

$$|\xi\rangle = \hat{S}(\xi)|0, 0\rangle = \sum_{n=0}^{\infty} c_n |n, n\rangle, \quad (4)$$

where  $c_n = e^{in\varphi} (\tanh r)^n / \cosh r$ . The average number of photons in either of the two modes is  $\langle n \rangle = \sinh^2 r$ .

The probability  $p_{nm}$  of finding  $n$  photons in the signal mode and  $m$  photons in the idler mode, before the sample, is thus  $p_{nm} = \delta_{nm} |c_n|^2$ , while the probability of finding  $m$  photons in the ancilla is  $|c_m|^2$ . After the sample is tested, the joint probability is  $p_{nm} = |c_m|^2 p_n^{(m)}$ , where  $p_n^{(m)}$  is the probability of counting  $n$  photons in the output probe beam for the input of  $m$  photons. The corresponding Fisher information for the estimation of the absorption  $\alpha$  is then, according to Eq. (1), since only  $p_n^{(m)}$  depends on  $\alpha$ ,

$$\begin{aligned} F(\alpha) &= \sum_{m=0}^{\infty} \sum_{n=0}^m \frac{1}{|c_m|^2 p_n^{(m)}} \left[ \frac{\partial |c_m|^2 p_n^{(m)}}{\partial \alpha} \right]^2 \\ &= \sum_{m=0}^{\infty} |c_m|^2 \sum_{n=0}^m \frac{1}{p_n^{(m)}} \left[ \frac{\partial p_n^{(m)}}{\partial \alpha} \right]^2 = \sum_{m=0}^{\infty} |c_m|^2 F^{(m)}(\alpha), \end{aligned} \quad (5)$$

where  $F^{(m)}(\alpha)$  is the Fisher information for a  $m$ -photons Fock state probing the absorbing sample, obtained through photon counting. One knows, however, that photon counting actually leads to the quantum Fisher information for a Fock state input [12, 13], so  $F^{(m)}(\alpha) = \mathcal{F}_Q^{(m)}(\alpha) = m/[\alpha(1-\alpha)]$ . Therefore,  $F(\alpha)$  is a weighted average of QFIs corresponding to Fock states:

$$F(\alpha) = \frac{\sum_{m=0}^{\infty} |c_m|^2 m}{\alpha(1-\alpha)} = \frac{\bar{n}}{\alpha(1-\alpha)}, \quad (6)$$

since the sum in the first term on the right-hand side of the above equation is the average number of photons  $\bar{n}$  in either the probe or the ancilla, before probing the sample. For the incoming two-mode squeezed state considered here,  $\bar{n} = \sinh^2 r$ . In Appendix A Eq. (A9), it is shown that the Fisher informa-

tion above coincides with the QFI of the probe + ancilla output state. Therefore,

$$\mathcal{F}_Q(\alpha) = \frac{\bar{n}}{\alpha(1-\alpha)}. \quad (7)$$

The Fisher information (6) coincides with the upper bound, derived in [11], on the QFI for the estimation of absorption, for any single-mode quantum state with mean photon number  $\bar{n}$ . This was done by replacing the absorption medium by a beam splitter, with transmissivity equal to the absorption coefficient, thus turning the open system dynamics into a unitary one, involving the two modes of the beam splitter. The corresponding quantum Fisher information should be an upper bound on the corresponding quantity for the open system, since having access to the environment should result in better precision of estimation of the absorption parameter [41]. Consequently, no single mode quantum state with a mean photon number  $\bar{n}$  can beat the precision reached with a bimodal squeezed vacuum state with the same mean photon number in the probe beam. This can be generalized to the system probe plus ancilla considered here. If one replaces the absorbing medium by a beam splitter, as done for the single-mode case, the system will have a unitary evolution, and therefore the ancilla would not play any role: the upper bound is the same as in the single-mode case! And it is reached by the two-mode squeezed state considered here, when the probe plus ancilla output is detected through joint photon counting.

Eq. (7) leads to two important conclusions:

- (i) Joint photon counting on probe and ancilla is an optimal measurement, leading to the QFI corresponding to the parameter  $\alpha$ ;
- (ii) The QFI related to the bimodal squeezed input state coincides with a Fock state QFI for which the photon number is replaced by  $\bar{n}$ .

The resulting bound for the precision  $\Delta\alpha$  in the estimation is given by Eq. (A2):

$$\Delta\alpha = \sqrt{\frac{\alpha(1-\alpha)}{\bar{n}}}, \quad (8)$$

setting  $\mathcal{N} = 1$  in Eq. (A2).

As shown in [12, 13], Fock states lead to the best precision in the estimation of the absorption, for a fixed photon number. This implies that, through the use of an ancillary system, and for a given average photon number of photons probing the sample, it is possible to achieve the best precision in the estimation of the parameter  $\alpha$ , outperforming not only the Gaussian states.

This interesting result stems from the perfect correlation of photon numbers of probe and ancilla, as shown in Eq. (4). Although the bimodal squeezed state describing the ancilla+probe system does not have a well-defined number of photons, photon counting on the ancilla tells us that a Fock state with the same number of photons probed the sample. The result of photon counting in the probe then allows one to get information about the parameter  $\alpha$  as if the input state of the

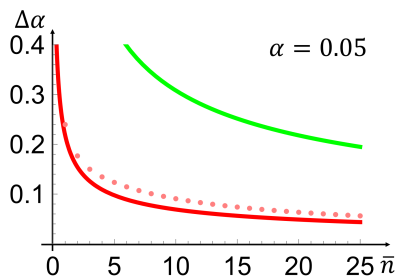


FIG. 2. Uncertainty in the estimation of the absorption constant, for  $\alpha = 0.05$ . Comparison between the bound for the uncertainty  $\Delta\alpha$  obtained from the quantum Fisher information for probe plus ancilla corresponding to two modes of an incoming bimodal squeezed state (red line) and the bound from the best single-mode Gaussian state [11] (pink dots), for the same average number of photons testing the absorption. The green line represents the standard limit, obtained for a single-mode coherent state testing the sample. For the probe plus ancilla setup with  $\bar{n} = 10$  the increase in precision from the standard limit is about 5 dB.

probe was a Fock state, leading to the best possible precision in the estimation of  $\alpha$ . Several runs of joint photon counting lead to quantum Fisher information of a Fock state for which the photon number is replaced by  $\bar{n}$ .

### A. Resilience of the joint photon counting procedure

The discussion above, stemming from the derivation of the Fisher information in Eq. (5), leads to important consequences: Any state, pure or mixed, with photon-number correlation between probe and ancilla could lead to Eq. (8). Not even entanglement is needed. Indeed, the following mixed product state of probe and ancilla,

$$\hat{\rho} = \sum_n p_n |n, n\rangle \langle n, n| \quad (9)$$

has the same QFI as a two-mode vacuum squeezed state with the same average number of photons. This implies that the preparation of the input state via OPA is resilient to phase noise. Furthermore, it also allows one to understand and generalize numerical results published in [6], where it was shown that the state  $|\psi\rangle_d = (1/d) \sum_{k=1}^d |k, k\rangle$  with  $3 \leq d \leq 6$  has the same QFI as a two-mode vacuum squeezed state with the same average number of photons, and that there are states with less entanglement than  $|\psi\rangle_d$  with similar performance.

### B. Quantum advantage of the probe+ancilla setup

Fig. 2 compares the result for  $\Delta\alpha$  obtained from the ancilla-based QFI Eq. (7) with the one corresponding to the best single-mode Gaussian state [11], which is a parameter-dependent squeezed and displaced vacuum state, for the same average number of photons probing the sample. The bound obtained from Eq. (6) prevails, as expected from a QFI for a Fock-state expression with photon number equal to  $\bar{n} =$

$\sinh^2 r$ . This result is in conformity with [6], which pointed out the non-optimal nature of single-mode Gaussian states. One should note that both the input state and the detection procedure in the probe plus ancilla setup do not depend on the (unknown) parameter to be estimated, which is not the case of the procedure in [11].

In Fig. 2, these results are compared with the standard limit, which corresponds to probing the sample with an incoming coherent state, with the same average number of photons as in the previous setups, and measuring the intensity of the field after its interaction with the sample. It can be derived from the corresponding single-mode quantum Fisher information [11]:

$$\Delta\alpha = \sqrt{\frac{1-\alpha}{\bar{n}_1}}, \quad (10)$$

where  $\bar{n}_1$  is the incoming average number of photons probing the sample. One should note that, for  $\alpha \rightarrow 1$ , that is, for strong absorption, one has  $\Delta\alpha \rightarrow 0$ . This is also the limit of vanishing outgoing intensity. Fig. 2 shows that, for  $\alpha = 0.05$  and  $\bar{n} = 10$ , the increase in precision from the standard limit is about 5 dB. In the limit of strong absorption,  $\alpha \rightarrow 1$ , both quantum Fisher information, for the single mode and the probe plus ancilla setups, converge to the standard limit, expressing the environment-induced emergence of classicality [82, 83]. This can be verified by comparing Eq. (8) and Eq. (10) when  $\alpha \rightarrow 1$ .

## III. TIME-REVERSAL STRATEGY

One should note, however, that joint photon counting is challenging, with present technologies. We show now that, for weak absorption, there is an interesting and useful alternative, which does not rely on joint photon counting, and involves a time-reversal detection scheme, illustrated in Fig. 3. It is based on a SU(1,1) interferometer [84–98], consisting of two OPAs, with the probed sample between them. The first one generates a two-mode squeezed state from a vacuum input, with the signal mode probing the sample, and the idler beam playing the role of an ancilla. The second OPA reverses the transformation implemented by the first one, so that, in the absence of photon losses, there is no outgoing field. The time-reversed operation can be carried out in many different ways [90–92]. The simplest is to have a  $\pi$  phase difference between the beams pumping the first and the second OPA. We assume that proper calibration compensates for the difference in optical paths of both arms due to the presence of the sample. Detection of the total number of outgoing photons leads to the estimation of the absorption, defined, as before, by the constant  $\alpha$ , so that, if  $I_1$  and  $I_2$  are the intensities of light in the upper arm of the interferometer, before and after the absorbing medium, then  $I_2 = (1 - \alpha)I_1$ . Fig. 3 displays the annihilation operators corresponding to the electromagnetic fields in several regions of the device. The relations between them are obtained from the squeezing transformations and the absorption.

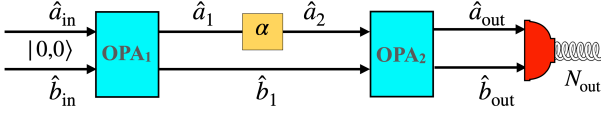


FIG. 3. Experimental SU(1,1) setup for squeezed vacuum time-reversal metrology. The absorption medium is placed between two optical parametric amplifiers (OPAs), on the upper arm of the interferometer. The first one, with vacuum input, produces a two-mode squeezed state, the signal beam probing the medium and the idler playing the role of an ancilla. The second OPA reverses the squeezing transformation, so that in the absence of the absorption medium, there is no outgoing field. Detection of the total number of outgoing photons leads to the estimation of the photon-loss coefficient  $\alpha$ .

Thus, from the first OPA, one has [81]

$$\begin{aligned}\hat{a}_1 &= \hat{a}_{\text{in}} \cosh r + \hat{b}_{\text{in}}^\dagger e^{i\phi} \sinh r, \\ \hat{b}_1 &= \hat{b}_{\text{in}} \cosh r + \hat{a}_{\text{in}}^\dagger e^{i\phi} \sinh r,\end{aligned}\quad (11)$$

where  $[\hat{a}_{\text{in}}, \hat{a}_{\text{in}}^\dagger] = 1$ ,  $[\hat{b}_{\text{in}}, \hat{b}_{\text{in}}^\dagger] = 1$  and the squeezing transformation is

$$\hat{S}(\xi) = \exp(\xi \hat{a}^\dagger \hat{b}^\dagger - \xi^* \hat{a} \hat{b}), \quad (12)$$

where  $\xi = r e^{i\phi}$  is the squeezing parameter, with  $\hat{a}_1 = \hat{S}^{-1} \hat{a}_{\text{in}} \hat{S}$ ,  $\hat{b}_1 = \hat{S}^{-1} \hat{b}_{\text{in}} \hat{S}$ .

The second OPA applies the time-reversed transformation ( $\xi \rightarrow -\xi$ ), resulting in the output operators (see Fig. 3):

$$\begin{aligned}\hat{a}_{\text{out}} &= \hat{a}_2 \cosh r - \hat{b}_1^\dagger e^{i\phi} \sinh r, \\ \hat{b}_{\text{out}} &= \hat{b}_1 \cosh r - \hat{a}_2^\dagger e^{i\phi} \sinh r.\end{aligned}\quad (13)$$

The photon loss, due to absorption and scattering, can be described by

$$\hat{a}_2 = \hat{a}_1 \sqrt{1 - \alpha} + \hat{c} \sqrt{\alpha}, \quad (14)$$

where  $\hat{c}$  stands for the annihilation operator corresponding to the vacuum noise mode. The presence of  $\hat{c}$  preserves the commutation relation of the field operators:  $[\hat{a}_2, \hat{a}_2^\dagger] = [\hat{a}_1, \hat{a}_1^\dagger] = 1$ .

From Eq. (11), Eq. (13), and Eq. (14), it follows that

$$\begin{aligned}\hat{a}_{\text{out}} &= \hat{a}_{\text{in}} (\cosh^2 r \sqrt{1 - \alpha} - \sinh^2 r) \\ &\quad - \hat{b}_{\text{in}}^\dagger e^{i\phi} \sinh r \cosh r (1 - \sqrt{1 - \alpha}) + \hat{c} \cosh r \sqrt{\alpha}, \\ \hat{b}_{\text{out}} &= \hat{b}_{\text{in}} (\cosh^2 r - \sinh^2 r \sqrt{1 - \alpha}) \\ &\quad + \hat{a}_{\text{in}}^\dagger e^{i\phi} \sinh r \cosh r (1 - \sqrt{1 - \alpha}) \\ &\quad - \hat{c}^\dagger e^{i\phi} \sinh r \sqrt{\alpha}.\end{aligned}\quad (15)$$

In the absence of the sample, it is easy to check that  $\hat{a}_{\text{out}} = \hat{a}_{\text{in}}$ ,  $\hat{b}_{\text{out}} = \hat{b}_{\text{in}}$ .

From Eq. (15), one gets the average total number of output

photons:

$$\begin{aligned}\bar{N}_{\text{out}} &= \langle \hat{a}_{\text{out}}^\dagger \hat{a}_{\text{out}} + \hat{b}_{\text{out}}^\dagger \hat{b}_{\text{out}} \rangle \\ &= 2 \sinh^2 r \cosh^2 r (1 - \sqrt{1 - \alpha})^2 + \alpha \sinh^2 r.\end{aligned}\quad (16)$$

The variance  $\Delta^2 N_{\text{out}}$  is displayed in Appendix B Eq. (B6).

We calculate  $\Delta\alpha$  through the sensitivity, which can be related in this case to photon number fluctuations:

$$\Delta\alpha = \frac{\Delta N_{\text{out}}}{|d\bar{N}_{\text{out}}/d\alpha|}, \quad (17)$$

where

$$\Delta^2 N_{\text{out}} = \langle (N_{\text{out}} - \bar{N}_{\text{out}})^2 \rangle \quad (18)$$

is the variance of the total number of photons.

From these expressions, the sensitivity can be calculated. Details are given in Appendix B Eqs. (B7) - (B9). The corresponding uncertainty is plotted in Fig. 4, and compared with the one obtained from the QFI in Eq. (7). For weak absorption, the result obtained from the time-reversal procedure is practically indistinguishable from the probe plus ancilla quantum Fisher information bound.

Since only the measurements of the total output photon number and its variance are needed here, they can be obtained through measurement of the intensity of photocurrents produced by the output fields and their cross-correlations, which does not require reconstructing the photon-number distribution [99].

In the next section, we demonstrate another advantage of this method: the resilience to moderate photon losses of the incoming probe plus the ancilla beam.

#### IV. RESILIENCE OF TIME-REVERSAL TO EXTRA PHOTON LOSSES

General optical parametric amplifiers (OPAs) can produce impure entanglement due to various factors, leading to a re-

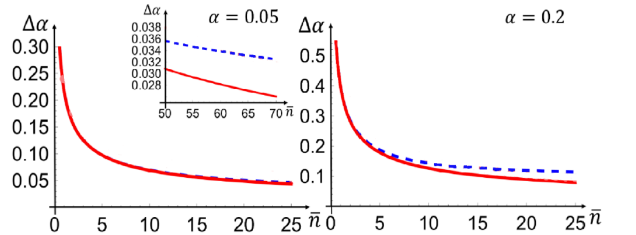


FIG. 4. Uncertainty bounds for probe plus ancilla QFI and SU(1,1) result. The uncertainty bounds from the quantum Fisher information corresponding to the probe and ancilla associated with the two modes of a bimodal squeezed state (red curve), given by Eq. (6), and the one resulting from a sensitive calculation for the total number of outgoing photons in the SU(1,1) setup illustrated in Fig. 3 (dashed blue line). For weak absorption ( $\alpha \ll 1$ ), results are practically indistinguishable for the range of  $\bar{n}$  considered here.

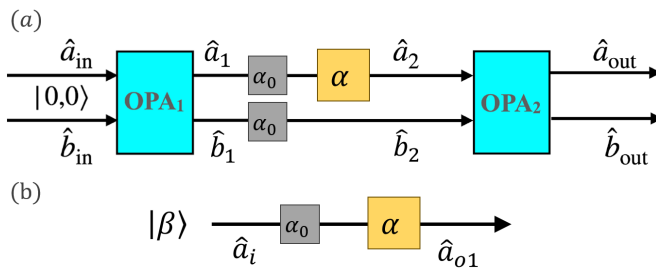


FIG. 5. (a). The impurity of the two-mode squeezed state generated by general optical parametric amplifiers is modeled by adding additional loss to the two-mode squeezed vacuum before passing through the sample  $\alpha$ . (b). For comparison, the corresponding sensing protocol with a coherent beam is shown.

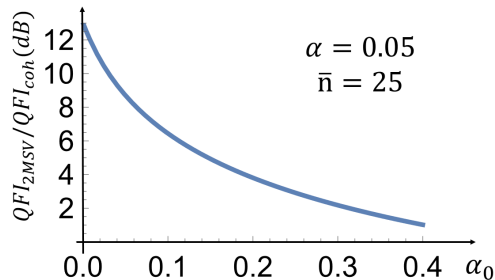


FIG. 6. The ratio between the quantum Fisher Informations corresponding to a two-mode squeezed vacuum (2MSV) and to a coherent state,  $QFI_{2MSV}/QFI_{coh}$ , in dB, for  $\alpha = 0.05$  and  $\bar{n} = 25$ , as a function of the impurity loss  $\alpha_0$ .

duction in the quality of the generated entanglement. We have already shown that the joint photon counting procedure is not affected if the input state becomes a mixture of photon-correlated probe plus ancilla states. We consider now the effect of extra photon losses.

It is worth noting that while losses can introduce impurities in the entanglement produced by general OPAs, it is still possible to have quantum gain for the joint photon counting and the time-reversal setup. In Fig. 5, additional loss is introduced to both modes of the two-mode squeezed vacuum before it passes through the sample. For simplicity, we assume the degree of loss  $\alpha_0$  to be the same for both modes. The calculations are similar to those in Appendix B.

As shown in Fig. 6, where the QFI for estimation of  $\alpha$  corresponding to the two-mode squeezed state is compared to the QFI for a single-mode coherent state input with the same additional loss  $\alpha_0$ , quantum advantage persists even after undergoing significant loss (advantage of 3 dB with  $\alpha_0 \sim 5\alpha$ ). This actually refers to the joint photon counting procedure, since the second OPA does not change the QFI.

The resilience of the time-reversal procedure to noise is illustrated in Fig. 7. Even for extra noise equal to the sample absorption constant, there is still significant advantage, as compared to the estimation corresponding to a coherent state input, subject to the same extra noise. This is an important and useful property of the time-reversal strategy proposed here.

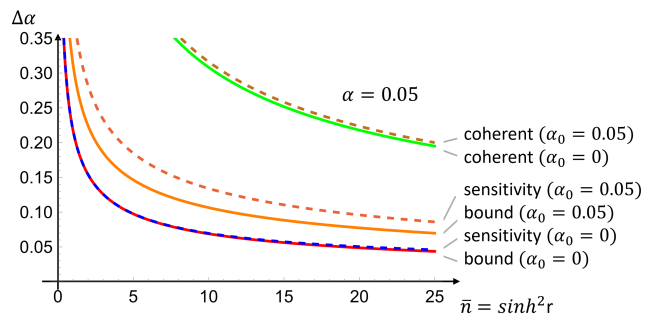


FIG. 7. Resilience of the time-reversal procedure: Precision  $\Delta\alpha$  in the estimation of the sample absorption constant as a function of the extra loss  $\alpha_0$  in both probe and conjugate beams, as in Fig. 5(a). For comparison, the standard quantum limit, corresponding to a single-mode coherent state input, as in Fig. 5(b), is also shown. The scale on x axis is the number of photons produced by the OPA in each beam.

## V. DISCUSSION

Optimal quantum sensing of open-system dynamics may require strategies that differ markedly from those applied to lossless systems. Entanglement of the probe with an ancilla may enhance the precision of estimation, even though the ancilla does not interact with the parameter-dependent system, a property that is absent for unitary dynamics. Here we have considered the estimation of photon loss for a light beam propagating in a sample or, more generally, of the loss coefficient in a bosonic channel, due to absorption or scattering by the sample.

The probe and ancilla are the modes of a bimodal squeezed state, produced by an optical parametric amplifier. We calculated the corresponding quantum Fisher information for estimation of the absorption coefficient and showed that the respective uncertainty bound coincides with the one for a Fock state, being saturated by joint photon counting for the outgoing probe and ancilla, a detection procedure that does not depend on the value of the parameter. The ancilla strategy benefits therefore from the extreme precision associated with Fock states of the probe, surpassing the sensing obtained with the best parameter-dependent single-mode Gaussian state [11], while overcoming the challenge of producing high photon-number eigenstates.

Joint photon counting is however challenging, with present technologies [7]. We have therefore described an approach that does not require this procedure. It is based on the conjunction of the ancilla strategy with a time-reversal strategy, implemented with a  $SU(1,1)$  interferometer consisting of two optical parametric amplifiers, so that the first one generates a two-mode squeezed state, corresponding to the probe and the ancilla, and the second one undoes the squeezing produced by the first one, after the probe has interacted with the sample. The addition of the second optical parametric amplifier does not change the quantum Fisher information, which is invariant under unitary transformations. An estimation based on a sensitivity relation for the total number of outgoing photons and its variance leads to an uncertainty in the absorption coefficient.

cient with a precision that is, for weak absorption, practically indistinguishable from the bound obtained from the quantum Fisher information for the probe plus ancilla system. This detection setup is also independent of the (unknown) parameter to be estimated, implying that phase stabilization and mode-matching for the two optical parametric amplifiers can be done once and for all: the device is then ready to be used, independently of the value of the parameter. Interestingly, quantum gain is still achieved for this protocol under moderate photon losses of the probe plus ancilla input beam, even for losses compared to the estimated absorption parameter.

The quantum advantage in the precision of estimation obtained with the ancilla and time-reversal strategy, demonstrated here, relies on available technology and opens the way to the increase in precision of a diversity of metrological tasks involving open systems.

#### APPENDIX A. QUANTUM FISHER INFORMATION OF ABSORPTION CONSTANT FOR THE TIME-REVERSED ANCILLA-BASED METROLOGY

We note that the two-mode squeezed state has a Gaussian Wigner function. It can be shown that if one of the modes goes through an absorber, the output is still a Gaussian Wigner function, though it corresponds to a mixed state of the output field [100]. The general method for calculating the quantum Fisher information (QFI) for a Gaussian system has been developed by [101–109]. We apply specifically the method in [109] to obtain the quantum Fisher information of the system described by Fig. 1. For a two-mode bosonic system, we may define a vector of annihilation and creation operators given by

$$\hat{A} = (a_1, a_2, a_1^\dagger, a_2^\dagger)^T. \quad (\text{A1})$$

Gaussian states can be fully characterized by their first moments (the displacement vector)  $d_m = \text{tr}[\rho \hat{A}_m]$  and the second moments (the covariance matrix)  $\sigma_{mn} = \text{tr}[\hat{\rho} \{\Delta \hat{A}_m, \Delta \hat{A}_n^\dagger\}]$ , where  $\Delta \hat{A} := \hat{A} - d$ . The subscripts  $m$  and  $n$  stand for the components of the vector defined in Eq. (A1). The QFI is given by

$$\mathcal{F}_Q(\alpha) = \lim_{v \rightarrow 1} \frac{1}{2} \text{vec} \left( \frac{\partial \sigma}{\partial \alpha} \right)^\dagger M^{-1} \text{vec} \left( \frac{\partial \sigma}{\partial \alpha} \right), \quad (\text{A2})$$

where the matrix  $M$  can be expressed by

$$M = v^2 \bar{\sigma} \otimes \sigma - K \otimes K, \quad (\text{A3})$$

for the system considered here, with a zero displacement vector. Other notations in Eq. (A2) include the symplectic form  $K = \text{diag}(1, 1, -1, -1)$ , and the operator  $\text{vec}(\Lambda)$ . Applying  $\text{vec}(\Lambda)$  on a matrix  $\Lambda = (\Lambda_1, \Lambda_2)$  will transform it to a vector  $\text{vec}(\Lambda) = (\Lambda_1^T, \Lambda_2^T)^T$ . Replacing the operators  $a_1$  and  $b_1$  in

Eq. (A1) by  $\hat{a}_{\text{out}}$  and  $\hat{b}_{\text{out}}$ , we obtain

$$\sigma = \begin{pmatrix} \langle \hat{a}_o \hat{a}_o^\dagger + \hat{a}_o^\dagger \hat{a}_o \rangle & 2 \langle \hat{a}_o \hat{b}_o^\dagger \rangle & 2 \langle \hat{a}_o \hat{a}_o \rangle & 2 \langle \hat{a}_o \hat{b}_o \rangle \\ 2 \langle \hat{a}_o^\dagger \hat{b}_o \rangle & \langle \hat{b}_o \hat{b}_o^\dagger + \hat{b}_o^\dagger \hat{b}_o \rangle & 2 \langle \hat{a}_o \hat{b}_o \rangle & 2 \langle \hat{b}_o \hat{b}_o \rangle \\ 2 \langle \hat{a}_o^\dagger \hat{a}_o \rangle & 2 \langle \hat{a}_o^\dagger \hat{b}_o \rangle & \langle \hat{a}_o^\dagger \hat{a}_o + \hat{a}_o \hat{a}_o^\dagger \rangle & 2 \langle \hat{a}_o^\dagger \hat{b}_o \rangle \\ 2 \langle \hat{a}_o^\dagger \hat{b}_o \rangle & 2 \langle \hat{b}_o^\dagger \hat{b}_o \rangle & 2 \langle \hat{a}_o \hat{b}_o \rangle & \langle \hat{b}_o^\dagger \hat{b}_o + \hat{b}_o \hat{b}_o^\dagger \rangle \end{pmatrix}, \quad (\text{A4})$$

where for brevity, we note  $\hat{a}_{\text{out}}$  and  $\hat{b}_{\text{out}}$  by  $\hat{a}_o$  and  $\hat{b}_o$ . These are given by

$$\begin{aligned} \hat{a}_o &= \hat{a}_1 \sqrt{1 - \alpha} + \hat{c} \sqrt{\alpha}, \\ \hat{b}_o &= \hat{b}_1, \end{aligned} \quad (\text{A5})$$

where  $\hat{a}_1$  and  $\hat{b}_1$  are given by Eq. (11). In the system considered here, many of the off-diagonal terms are zero

$$\begin{aligned} \langle \hat{a}_o \hat{a}_o \rangle &= \langle \hat{a}_o^\dagger \hat{a}_o^\dagger \rangle = \langle \hat{b}_o \hat{b}_o \rangle = \langle \hat{b}_o^\dagger \hat{b}_o^\dagger \rangle \\ &= \langle \hat{a}_o \hat{b}_o^\dagger \rangle = \langle \hat{a}_o^\dagger \hat{b}_o \rangle = 0. \end{aligned} \quad (\text{A6})$$

Thus, we obtain

$$\sigma = \begin{pmatrix} 2 \langle \hat{a}_o^\dagger \hat{a}_o \rangle + 1 & 0 & 0 & 2 \langle \hat{a}_o \hat{b}_o \rangle \\ 0 & 2 \langle \hat{b}_o^\dagger \hat{b}_o \rangle + 1 & 2 \langle \hat{a}_o \hat{b}_o \rangle & 0 \\ 0 & 2 \langle \hat{a}_o^\dagger \hat{b}_o \rangle & 2 \langle \hat{a}_o^\dagger \hat{a}_o \rangle + 1 & 0 \\ 2 \langle \hat{a}_o^\dagger \hat{b}_o \rangle & 0 & 0 & 2 \langle \hat{b}_o^\dagger \hat{b}_o \rangle + 1 \end{pmatrix}, \quad (\text{A7})$$

where

$$\begin{aligned} \langle \hat{a}_o^\dagger \hat{a}_o \rangle &= (1 - \alpha) \sinh^2 r, \\ \langle \hat{b}_o^\dagger \hat{b}_o \rangle &= \sinh^2 r, \\ \langle \hat{a}_o \hat{b}_o \rangle &= \langle \hat{b}_o \hat{a}_o \rangle = e^{i\phi} \sinh r \cosh r \sqrt{1 - \alpha}, \\ \langle \hat{a}_o^\dagger \hat{b}_o \rangle &= \langle \hat{b}_o^\dagger \hat{a}_o \rangle = e^{-i\phi} \sinh r \cosh r \sqrt{1 - \alpha}. \end{aligned} \quad (\text{A8})$$

From Eq. (A2), Eq. (A6), and Eq. (A7), we obtain the quantum Fisher information corresponding to the absorption constant  $\alpha$ , for the ancilla-based metrology,

$$\mathcal{F}_Q(\alpha) = \frac{\sinh^2 r}{\alpha(1 - \alpha)}, \quad (\text{A9})$$

which coincides with Eq. (6) of the main text. We note that this result can be derived from the quantum Fisher information obtained in [6], where it was shown that input two-mode squeezed states outperform any other class of Gaussian states, for the estimation of the time-dependent parameter  $\gamma = \Gamma t$ , where  $\Gamma$  is the coupling of the channel to a thermal reservoir. The connection with Fock states, through the expression Eq. (A9), was not discussed there, as well as the resilience of these states against additional noise, which are direct consequences of our derivation method in the main text. Since the time-reversal procedure is a unitary transformation, which does not change the quantum Fisher information, Eq. (A9) also applies to the time-reversed ancilla system. This can be

checked explicitly for the arrangement of Fig. 3 for which  $\hat{a}_{\text{out}}$  and  $\hat{b}_{\text{out}}$  are given by Eq. (15). We can derive

$$\begin{aligned}
\langle \hat{a}_o^\dagger \hat{a}_o \rangle &= \sinh^2 r \cosh^2 r (1 - \sqrt{1 - \alpha})^2, \\
\langle \hat{b}_o^\dagger \hat{b}_o \rangle &= \sinh^2 r \cosh^2 r (1 - \sqrt{1 - \alpha})^2 + \alpha \sinh^2 r, \\
\langle \hat{a}_o \hat{b}_o \rangle &= \langle \hat{b}_o \hat{a}_o \rangle = -e^{i\phi} \sinh r \cosh r (1 - \sqrt{1 - \alpha}) \\
&\quad \times (\cosh^2 r - \sinh^2 r \sqrt{1 - \alpha}), \\
\langle \hat{a}_o^\dagger \hat{b}_o^\dagger \rangle &= -e^{-i\phi} \sinh r \cosh r (1 - \sqrt{1 - \alpha}) \\
&\quad \times (\cosh^2 r - \sinh^2 r \sqrt{1 - \alpha}).
\end{aligned} \tag{A10}$$

On substituting Eq. (A10) in Eq. (A7) and using Eq. (A2) and Eq. (A3), we do obtain Eq. (A9).

## APPENDIX B. SENSITIVITY FOR THE TIME-REVERSED SCHEME

Here we present the expressions needed for the evaluation of  $\Delta\alpha$  in Eq. (17). For simplicity, we express Eq. (15) in the main text as

$$\begin{aligned}
\hat{a}_{\text{out}} &= c_{11}\hat{a}_{\text{in}} + c_{12}\hat{b}_{\text{in}}^\dagger + c_{13}\hat{c}, \\
\hat{b}_{\text{out}} &= c_{21}\hat{a}_{\text{in}}^\dagger + c_{22}\hat{b}_{\text{in}} + c_{23}\hat{c}^\dagger,
\end{aligned} \tag{B1}$$

where  $c_{11}$ ,  $c_{12}$ ,  $c_{13}$ ,  $c_{21}$ ,  $c_{22}$ , and  $c_{23}$  are given by

$$\begin{aligned}
c_{11} &= \sqrt{1 - \alpha} \cosh^2 r - \sinh^2 r, \\
c_{12} &= -(1 - \sqrt{1 - \alpha})e^{i\phi} \cosh r \sinh r, \\
c_{13} &= \cosh r \sqrt{\alpha}, \\
c_{21} &= (1 - \sqrt{1 - \alpha})e^{i\phi} \cosh r \sinh r, \\
c_{22} &= \cosh^2 r - \sqrt{1 - \alpha} \sinh^2 r, \\
c_{23} &= -e^{i\phi} \sinh r \sqrt{\alpha}.
\end{aligned} \tag{B2}$$

We obtain the average total number of output photons

$$\bar{N}_{\text{out}} = \langle \hat{a}_{\text{out}}^\dagger \hat{a}_{\text{out}} + \hat{b}_{\text{out}}^\dagger \hat{b}_{\text{out}} \rangle = |c_{12}|^2 + |c_{21}|^2 + |c_{23}|^2, \tag{B3}$$

and its variance

$$\begin{aligned}
\Delta^2 N_{\text{out}} &= \langle (N_{\text{out}} - \bar{N}_{\text{out}})^2 \rangle \\
&= |c_{12}|^2 (|c_{11}|^2 + |c_{13}|^2 + |c_{22}|^2) + |c_{22}|^2 |c_{23}|^2 \\
&\quad + 2|c_{12}c_{22}(c_{11}c_{21} + c_{13}c_{23})|.
\end{aligned} \tag{B4}$$

Defining  $\eta := (1 - \sqrt{1 - \alpha})$ , we obtain

$$\frac{d\bar{N}_{\text{out}}}{d\alpha} = 2 \cosh^2 r \sinh^2 r \frac{\eta}{1 - \eta} + \sinh^2 r, \tag{B5}$$

and

$$\begin{aligned}
\Delta^2 N_{\text{out}} &= \eta^2 \cosh^2 r (2\eta - 1 + 3\eta^2 \cosh^2 r \sinh^2 r) \\
&\quad + 2\alpha\eta \cosh^2 r (1 + \eta \sinh^2 r) \\
&\quad + (1 + \eta \sinh^2 r)^2 (2\eta \cosh^2 r - \alpha \sinh^2 r).
\end{aligned} \tag{B6}$$

From these expressions, the sensitivity can be calculated.

$$\Delta\alpha = \frac{\sqrt{A}}{B}, \tag{B7}$$

where

$$\begin{aligned}
A &= \eta^2 (\bar{n} + 1) [2\eta - 1 + 3\eta^2 (\bar{n} + 1)\bar{n}] \\
&\quad + 2\alpha\eta (\bar{n} + 1) (1 + \eta\bar{n}) \\
&\quad + (1 + \eta\bar{n})^2 [2\eta(\bar{n} + 1) - \alpha\bar{n}],
\end{aligned} \tag{B8}$$

and

$$B = \sqrt{\bar{n}} \left[ 1 + \frac{2\eta}{\sqrt{1 - \alpha}} (\bar{n} + 1) \right], \tag{B9}$$

in terms of the average number of photons interacting with the sample,  $\bar{n} = \langle \hat{a}_1^\dagger \hat{a}_1 \rangle = \sinh^2 r$ , and  $\eta := (1 - \sqrt{1 - \alpha})$ . For small values of  $\alpha$  such that  $\alpha \ll 1$  and  $\alpha\bar{n} \lesssim 1$ , Eq. (B7) can be expanded to

$$\Delta\alpha = \frac{\sqrt{\alpha} [1 + \alpha\bar{n} + \frac{1}{8}\alpha^3\bar{n}^3 + \frac{1}{2}\alpha(1 + \frac{1}{2}\alpha\bar{n} + \frac{1}{2}\alpha^2\bar{n}^2)]}{\sqrt{\bar{n}} [1 + \alpha\bar{n} + \alpha(1 + \frac{3}{4}\alpha\bar{n})]}, \tag{B10}$$

where the leading term is  $\Delta\alpha \sim \sqrt{\alpha/\bar{n}}$ , showing that the SU(1, 1) sensitivity estimate goes over the result in Eq. (8), for  $\alpha \ll 1$ .

## VI. ACKNOWLEDGMENTS

G.S.A and J.W. are grateful for the support of Air Force Office of Scientific Research (Award No. FA-9550-20-1-0366) and the Robert A. Welch Foundation (A-1943-20210327). R.L.M.F. and L.D. acknowledge the support of the Brazilian agencies CNPq, CAPES, and the Rio de Janeiro State Foundation for Research Support (FAPERJ). R. L. M. F. acknowledges the support of the John Templeton Foundation (Grant 62424). L.D. acknowledges the support by the National Science Foundation under Grants No. NSF PHY-1748958 and PHY-2309135.

[1] C. W. Helstrom, "Quantum Detection and Estimation Theory," Chap. VIII.4, Academic Press, New York (1976).

[2] A. S. Holevo, "Probabilistic and Statistical Aspects of Quantum Theory," North-Holland, Amsterdam (1982).



- [3] C. L. Degen, F. Reinhard, and P. Cappellaro, "Quantum sensing", *Rev. of Mod. Phys.* **89**, 035002 (2017).
- [4] A. Fujiwara, "Quantum channel identification problem," *Phys. Rev. A* **63**, 042304 (2001).
- [5] A. Fujiwara, "Estimation of a generalized amplitude-damping channel," *Phys. Rev. A* **70**, 012317 (2004).
- [6] A. Monras and F. Illuminati, "Measurement of damping and temperature: Precision bounds in Gaussian dissipative channels," *Phys. Rev. A* **83**, 012315 (2011).
- [7] R. Nair, "Quantum-limited loss sensing: Multiparameter estimation and Bures distance between loss channels," *Phys. Rev. Lett.* **121**, 230801 (2018).
- [8] Z. Gong, C. N. Gagatsos, S. Guha, *et al.*, "Fundamental Limits of Loss Sensing over Bosonic Channels," 2021 IEEE International Symposium on Information Theory (ISIT), pp. 1182-1187 (2021).
- [9] P.-A. Moreau, J. Sabines-Chesterking, R. Whittaker, *et al.*, "Demonstrating an absolute quantum advantage in direct absorption measurement," *Sci. Rep.* **7**, 6256 (2017).
- [10] E. Losero, I. Ruo-Berchera, A. Meda, *et al.*, "Unbiased estimation of an optical loss at the ultimate quantum limit with twin-beams," *Sci. Rep.* **8**, 7431 (2018).
- [11] A. Monras and M. G. A. Paris, "Optimal quantum estimation of loss in bosonic channels," *Phys. Rev. Lett.* **98**, 160401 (2007).
- [12] G. Adesso, F. Dell'Anno, S. De Siena, *et al.*, "Optical estimation of losses at the ultimate quantum limit with non-Gaussian states," *Phys. Rev. A* **79**, 040305(R) (2009).
- [13] J. Wang, L. Davidovich, and G. S. Agarwal, "Quantum sensing of open systems: Estimation of damping constants and temperature," *Phys. Rev. Research* **2**, 033389 (2020).
- [14] T. J. Sturges *et al.*, "Quantum simulations with multiphoton Fock states," *npj Quantum Information* [7, 91 (2021)].
- [15] F. Toscano, D. A. R. Dalvit, L. Davidovich, *et al.*, "Sub-Planck phase-space structures and Heisenberg-limited measurements," *Phys. Rev. A* **73**, 023803 (2006).
- [16] M. Penasa, S. Gerlich, T. Rybarczyk, *et al.*, "Measurement of a microwave field amplitude beyond the standard quantum limit," *Phys. Rev. A* **94**, 022313 (2016).
- [17] S. C. Burd, R. Srinivas, J. J. Bollinger, *et al.*, "Quantum amplification of mechanical oscillator motion," *Science* **364**, 1163 (2019).
- [18] G. S. Agarwal and L. Davidovich, "Quantifying quantum-amplified metrology via Fisher information," *Phys. Rev. Research* **4**, L012014 (2022).
- [19] T. Macri, A. Smerzi, and L. Pezzè, "Loschmidt echo for quantum metrology," *Phys. Rev. A* **94**, 010102 (2016).
- [20] S. P. Nolan, S. S. Szigeti, and S. A. Haine "Optimal and robust quantum metrology using interaction-based readouts," *Phys. Rev. Lett.* **119**, 193601 (2017).
- [21] S. Colombo, E. Pedrozo-Peñafiel, A. F. Adiyatullin, *et al.*, "Time-reversal-based quantum metrology with many-body entangled states," *Nat. Phys.* **18**, 925 (2022).
- [22] D. Linnemann, H. Strobel, W. Muessel, *et al.*, "Quantum-Enhanced Sensing Based on Time Reversal of Nonlinear Dynamics," *Phys. Rev. Lett.* **117**, 013001 (2016).
- [23] Michael A. Armen, John K. Au, John K. Stockton, Andrew C. Doherty, and Hideo Mabuchi, "Adaptive homodyne measurement of optical phase," *Phys. Rev. Lett.* **89**, 133602 (2002).
- [24] T. A. Wheatley *et al.*, "Adaptive optical phase estimation using time-symmetric quantum smoothing," *Phys. Rev. Lett.* **104**, 093601 (2010).
- [25] A. A. Berni *et al.*, "Ab initio quantum-enhanced optical phase estimation using real-time feedback control," *Nature Photonics* **9**, 577 (2015).
- [26] Neil B. Lovett, Cécile Crosnier, Martí Perarnau-Llobet, and Barry C. Sanders, "Differential evolution for many-particle adaptive quantum metrology," *Phys. Rev. Lett.* **110**, 220501 (2013).
- [27] Alexander Hentschel and Barry C. Sanders, "Efficient algorithm for optimizing adaptive quantum metrology processes," *Phys. Rev. Lett.* **107**, 233601 (2011).
- [28] H. Cramér, "Mathematical Methods of Statistics," p. 500, Princeton University, Princeton, NJ, USA (1946).
- [29] R. A. Fisher, "On the dominance ratio," *Proc. R. Soc. Edinburgh* **42**, 321 (1922).
- [30] S. L. Braunstein and C. M. Caves, "Statistical distance and the geometry of quantum states," *Phys. Rev. Lett.* **72**, 3439 (1994).
- [31] C. W. Helstrom, "Simultaneous measurement from the standpoint of quantum estimation theory," *Found. Phys.* **4**, 453 (1974).
- [32] C. M. Caves, "Quantum-mechanical noise in an interferometer," *Phys. Rev. D* **23**, 1693 (1981).
- [33] S. P. Walborn, A. H. Pimentel, L. Davidovich, *et al.* "Quantum-enhanced sensing from hyperentanglement", *Phys. Rev. A* **97**, 010301 (2018).
- [34] D. Mason, J. Chen, M. Rossi, *et al.*, "Continuous force and displacement measurement below the standard quantum limit," *Nat. Phys.* **15**, 745 (2019).
- [35] K. A. Gilmore, M. Affolter, R. J. Lewis-Swan, *et al.*, "Quantum-enhanced sensing of displacements and electric fields with two-dimensional trapped-ion crystals," *Science* **373**, 673 (2021).
- [36] A. S. Holevo, "Covariant measurements and uncertainty relations," *Rep. Math. Phys.* **16**, 385 (1979).
- [37] A. Monras, "Optical phase measurements with pure Gaussian states," *Phys. Rev. A* **73**, 033821 (2006).
- [38] M. G. A. Paris, "Quantum estimation for quantum technology," *Int. J. Quantum Inf.* **7**, 125 (2009).
- [39] V. Giovannetti, S. Lloyd, and L. Maccone, "Advances in quantum metrology," *Nat. Photonics* **5**, 222 (2011).
- [40] R. Demkowicz-Dobrzański, M. Jarzyna, and J. Kolodyński, "Quantum limits in optical interferometry," *Prog. Opt.* **60**, 345 (2015).
- [41] B. M. Escher, R. L. de Matos Filho, and L. Davidovich, "General framework for estimating the ultimate precision limit in noisy quantum-enhanced metrology," *Nat. Phys.* **7**, 406 (2011).
- [42] E. Roccia, V. Cimini, M. Sbroscia, *et al.*, "Multiparameter approach to quantum phase estimation with limited visibility," *Optica* **5**, 1171 (2018).
- [43] C. L. Latune, B. M. Escher, R. L. de Matos Filho, *et al.*, "Quantum limit for the measurement of a classical force coupled to a noisy quantum-mechanical oscillator," *Phys. Rev. A* **88**, 042112 (2013).
- [44] A. Facon, E.-K. Dietsche, D. Grosso, *et al.*, "A sensitive electrometer based on a Rydberg atom in a Schrodinger-cat state," *Nature* **535**, 262 (2016).
- [45] G. T. Gillies and C. S. Unnikrishnan, "The attracting masses in measurements of G: an overview of physical characteristics and performance," *Philos. Trans. R. Soc. A* **372**, 20140022 (2014).
- [46] S. Qvarfort, A. Douglas K. Plato, D. Edward Bruschi, *et al.*, "Optimal estimation of time-dependent gravitational fields with quantum optomechanical systems," *Phys. Rev. Res.* **3**, 013159 (2021).
- [47] T. Westphal, H. Hepach, J. Pfaff, *et al.*, "Measurement of gravitational coupling between millimetre-sized masses," *Nature*

- 591, 225 (2021).
- [48] G. J. Milburn, W. -Y. Chen, and K. R. Jones, "Hyperbolic phase and squeeze-parameter estimation," *Phys. Rev. A* **50**, 801 (1994).
- [49] G. Chiribella, G. M. D'Ariano, and M. F. Sacchi, "Optimal estimation of squeezing," *Phys. Rev. A* **73**, 062103 (2006).
- [50] B. Stray, A. Lamb, A. Kaushik, *et al.*, "Quantum sensing for gravity cartography," *Nature* **602**, 590 (2022).
- [51] Z. Yu, B. Fang, L. Chen, *et al.*, "Memory-assisted quantum accelerometer with multi-bandwidth," *Photon. Res.* **10**, 1022-1030 (2022).
- [52] Y. -J. Chen, A. Hansen, G. W. Hoth, *et al.*, "Single-source multi-axis cold-atom interferometer in a centimeter-scale cell," *Phys. Rev. Applied* **12**, 014019 (2019).
- [53] J. S. Bennett, B. E. Vyhalek, H. Greenall, *et al.*, "Precision magnetometers for aerospace applications: a review," *Sensors* **21**, 5568 (2021).
- [54] T. Li, F. Li, X. Liu, *et al.*, "Quantum-enhanced stimulated Brillouin scattering spectroscopy and imaging," *Optica* **9**, 959 (2022).
- [55] R. Abbott, T. D. Abbott, S. Abraham, *et al.*, "Observation of gravitational waves from two neutron star-black hole coalescences," *ApJL* **915** L5 (2021).
- [56] T. Bothwell, C. J. Kennedy, A. Aeppli, *et al.*, "Resolving the gravitational redshift across a millimetre-scale atomic sample," *Nature* **602**, 420 (2022).
- [57] S. L. Braunstein, C. M. Caves, and G. J. Milburn, "Generalized uncertainty relations: Theory, examples, and Lorentz invariance," *Annals of Physics* **247**, 135 (1996).
- [58] J. Anandan and Y. Aharonov, "Geometry of quantum evolution," *Phys. Rev. Lett.* **65**, 1697 (1990).
- [59] M. M. Taddei, B. M. Escher, L. Davidovich, *et al.*, "Quantum speed limit for physical processes," *Phys. Rev. Lett.* **110**, 050402 (2013).
- [60] B. M. Escher, L. Davidovich, N. Zagury, *et al.*, "Quantum metrological limits via a variational approach," *Phys. Rev. Lett.* **109**, 190404 (2012).
- [61] R. Demkowicz-Dobrzański, J. Kolodyński, and M. Guță, "The elusive Heisenberg limit in quantum-enhanced metrology," *Nat. Comm.* **3**, 1063 (2012).
- [62] L. Banchi, S. L. Braunstein, and S. Pirandola, "Quantum fidelity for arbitrary Gaussian states," *Phys. Rev. Lett.* **115**, 260501 (2015).
- [63] R. Nichols, P. Liuzzo-Scorpo, P. A. Knott, *et al.*, "Multiparameter Gaussian quantum metrology," *Phys. Rev. A* **98**, 012114 (2018).
- [64] D. Šafránek, "Estimation of Gaussian quantum states," *J. Phys. A: Math. Theor.* **52**, 035304 (2019).
- [65] A. Acín, E. Jane, and G. Vidal, "Optimal estimation of quantum dynamics," **64**, 050302(R) (2001).
- [66] G. M. D'Ariano, P. L. Presti, and M. G. A. Paris, "Using Entanglement Improves the Precision of Quantum Measurements," *Phys. Rev. Lett.* **87**, 270404 (2001).
- [67] M. F. Sacchi, "Entanglement can enhance the distinguishability of entanglement-breaking channels," *Phys. Rev. A* **72**, 014305 (2005).
- [68] G. Wang and M. Ying, "Unambiguous discrimination among quantum operations," *Phys. Rev. A* **73**, 042301 (2006).
- [69] R. Demkowicz-Dobrzański and J. Kolodyński, "Efficient tools for quantum metrology with uncorrelated noise," *New J. Phys.* **15**, 073043 (2013).
- [70] R. Demkowicz-Dobrzański and L. Maccone, "Using entanglement against noise in quantum metrology," *Phys. Rev. Lett.* **113**, 250801 (2014).
- [71] Z. Huang, C. Macchiavello, and L. Maccone, "Usefulness of entanglement-assisted quantum metrology," *Phys. Rev. A* **94**, 012101 (2016).
- [72] S. Pirandola, R. Laurenza, C. Lupo, *et al.*, "Fundamental limits to quantum channel discrimination," *npj Quantum Inf.* **5**, 50 (2019).
- [73] W. Dür, M. Skotiniotis, F. Fröwis, *et al.*, "Improved quantum metrology using quantum error correction," *Phys. Rev. Lett.* **112**, 080801 (2014).
- [74] G. Arrad, Y. Vinkler, D. Aharonov, *et al.*, "Increasing sensing resolution with error correction," *Phys. Rev. Lett.* **112**, 150801 (2014).
- [75] E. M. Kessler, I. Lovchinsky, A. O. Sushkov, *et al.*, "Quantum error correction for metrology," *Phys. Rev. Lett.* **112**, 150802 (2014).
- [76] F. Li, T. Li, M. O. Scully, *et al.*, "Quantum Advantage with Seeded Squeezed Light for Absorption Measurement," *Phys. Rev. Applied* **15**, 044030 (2021).
- [77] G. Brida, M. Genovese and I. Ruo Berchera, "Experimental realization of sub-shot-noise quantum imaging," *Nat. Photon* **4**(4), 227-230 (2010).
- [78] Z. Zhang, S. Mouradian, F. N. C. Wong, *et al.*, "Entanglement-enhanced sensing in a lossy and noisy environment," *Phys. Rev. Lett.* **114**, 110506 (2015).
- [79] C. Ioannou, R. Nair, I. Fernandez-Corbaton, *et al.*, "Optimal circular dichroism sensing with quantum light: Multiparameter estimation approach," *Phys. Rev. A* **104**, 052615 (2021).
- [80] J. Wang and G. S. Agarwal, "Quantum Fisher information bounds on precision limits of circular dichroism," *Phys. Rev. A* **104**, 062613 (2021).
- [81] G. S. Agarwal, "Quantum Optics," Cambridge University Press, Chapter 3 (2013).
- [82] W. H. Zurek, "Decoherence, einselection, and the quantum origins of the classical," *Rev. Mod. Phys.* **75**, 715 (2003).
- [83] L. Davidovich, "From quantum to classical: Schrödinger cats, entanglement, and decoherence," *Physica Scripta* **91**, 063013 (2016).
- [84] B. Yurke, S. L. McCall, and J. R. Klauder, "SU(2) and SU(1,1) interferometers," *Phys. Rev. A* **33**, 4033 (1986).
- [85] W. N. Plick, J. P. Dowling, and G. S. Agarwal, "Coherent-light-boosted, sub-shot noise, quantum interferometry," *New Journal of Physics*, **12**, 083014 (2010).
- [86] A. M. Marino, N. V. Corzo Trejo, and P. D. Lett, "Effect of losses on the performance of an SU(1,1) interferometer," *Phys. Rev. A* **86**, 023844 (2012).
- [87] J. Xin, H. Wang, and J. Jing, "The effect of losses on the quantum-noise cancellation in the SU(1,1) interferometer," *Appl. Phys. Lett.* **109**, 051107 (2016).
- [88] S. S. Szigeti, R. J. Lewis-Swan, and S. A. Haine, "Pumped-up SU(1,1) interferometry," *Phys. Rev. Lett.* **118**, 150401 (2017).
- [89] M. Manceau, G. Leuchs, F. Khalili, *et al.*, "Detection loss tolerant supersensitive phase measurement with an SU(1,1) interferometer," *Phys. Rev. Lett.* **119**, 223604 (2017).
- [90] S. Liu, Y. Lou, J. Xin, *et al.*, "Quantum Enhancement of Phase Sensitivity for the Bright-Seeded SU(1,1) Interferometer with Direct Intensity Detection," *Phys. Rev. Applied* **10**, 064046 (2018).
- [91] Y. Liu, J. Li, L. Cui, *et al.*, "Loss-tolerant quantum dense metrology with SU(1,1) interferometer," *Opt. Express* **26**, 27705 (2018).
- [92] J. Qin, Y.-H. Deng, H.-S. Zhong, *et al.*, "Unconditional and Robust Quantum Metrological Advantage beyond N00N States," *Phys. Rev. Lett.* **130**, 070801 (2023).

- [93] S. Adhikari, N. Bhusal, C. You, *et al.*, "Phase estimation in an SU(1,1) interferometer with displaced squeezed states," *OSA Continuum* **1**, 438 (2018).
- [94] Y. Liu, N. Huo, J. Li, *et al.*, "Optimum quantum resource distribution for phase measurement and quantum information tapping in a dual-beam SU(1,1) interferometer," *Opt. Express* **27**, 11292 (2019).
- [95] L. Cui, J. Su, J. Li, *et al.*, "Quantum state engineering by nonlinear quantum interference," *Phys. Rev. A* **102**, 033718 (2020).
- [96] Z. Y. Ou and X. Li, "Quantum SU(1,1) interferometers: Basic principles and applications," *APL Photonics* **5**, 080902 (2020).
- [97] N. Huo, L. Cui, Y. Zhang, *et al.*, "Measurement-dependent erasure of distinguishability for the observation of interference in an unbalanced SU(1,1) interferometer," *PRX Quantum* **3**, 020313 (2022).
- [98] M. Kalash, and M. V. Chekhova, "Wigner function tomography via optical parametric amplification," *Optica* **10**, 1142 (2023).
- [99] L. Mandel and E. Wolf, "Optical Coherence and Quantum Optics," Cambridge University Press, Sec. 9.4 (1995).
- [100] G. Agarwal, "Wigner-function description of quantum noise in interferometers," *J. Mod. Opt.* **34**, 909 (1987).
- [101] O. Pinel, J. Fade, D. Braun, *et al.*, "Ultimate sensitivity of precision measurements with intense Gaussian quantum light: A multimodal approach," *Phys. Rev. A* **85**, 010101 (2012).
- [102] O. Pinel, P. Jian, N. Treps, *et al.*, "Quantum parameter estimation using general single-mode Gaussian states," *Phys. Rev. A* **88**, 040102 (2013).
- [103] Y. Gao and H. Lee, "Bounds on quantum multiple-parameter estimation with Gaussian state," *Eur. Phys. J. D* **68**, 1 (2014).
- [104] N. Friis, M. Skotiniotis, I. Fuentes, *et al.*, "Heisenberg scaling in Gaussian quantum metrology," *Phys. Rev. A* **92**, 022106 (2015).
- [105] D. Šafránek, A. R. Lee, and I. Fuentes, "Quantum parameter estimation using multi-mode Gaussian states," *New J. Phys* **17**, 073016 (2015).
- [106] L. Banchi, S. L. Braunstein, and S. Pirandola, "Quantum fidelity for arbitrary Gaussian states," *Phys. Rev. Lett.* **115**, 260501 (2015).
- [107] P. Marian and T. A. Marian, "Quantum Fisher information on two manifolds of two-mode Gaussian states," *Phys. Rev. A* **93**, 052330 (2016).
- [108] R. Nichols, P. Liuzzo-Scorpo, P. A. Knott, *et al.*, "Multiparameter Gaussian quantum metrology," *Phys. Rev. A* **98**, 012114 (2018).
- [109] D. Šafránek, "Estimation of Gaussian quantum states," *J. Phys. A: Math. Theor.* **52**, 035304 (2018).